

## Recent Advances in Optical Switches Using Silica-based PLC Technology

*Masayuki Okuno<sup>†</sup>, Takashi Goh, Shunichi Sohma, and Tomohiro Shibata*

### Abstract

We review recent progress in optical switches based on planar lightwave circuit (PLC) technology. First, we describe the basic configuration and fabrication of silica-based PLC switches. Then, we describe the configuration and characteristics of  $N \times N$  strictly nonblocking matrix switches (mainly a  $16 \times 16$  switch),  $1 \times N$  switches (mainly a  $1 \times 128$  switch), a  $128 \times 128$  switching sub-system consisting of 256  $1 \times 128$  switch modules, and an optical add/drop multiplexing circuit consisting of arrayed waveguide gratings and  $2 \times 2$  switches. We also report a low power consumption trial for large-scale PLC switches and the results of reliability tests.

### 1. Introduction

To handle the increase in Internet traffic, the bit rate of time division multiplexing (TDM) systems has increased rapidly and wavelength division multiplexing (WDM) systems have been introduced. To date, WDM systems have mainly been employed in point-to-point transmission systems. In such cases, the signals are processed in the system nodes after optical-electrical (O-E) conversion. This O-E conversion limits the throughput and increases the hardware cost. Optical nodes such as optical cross-connect (OXC) and optical add/drop multiplexing (OADM) nodes handle signals in the optical path layer; they are transparent as hardware and provide a high throughput [1]. Space division optical switches are key devices in these systems, and many types of switches including micro-electro-mechanical systems (MEMS) [2], bubble [3]-[4], and planar lightwave circuit (PLC) type switches have been developed.

At NTT Photonics Laboratories, we have been developing optical switches using silica-based PLC technology since the 1980s. A silica-based PLC is essentially a passive device. However, it can be used

to realize an optical switch by combining the thermo-optic (TO) effect and an interferometer configuration. PLC switches have low insertion loss and polarization dependence, are easy to attach to fibers, and are suitable for mass production. They are also stable and highly reliable. Many switches have been developed, and  $2 \times 2$  and  $8 \times 8$  matrix switches are already being marketed by an NTT group company. Currently, PLC switches capable of large-scale integration and offering high performance levels are attracting considerable attention because of the wavelength increase of WDM systems, and we have expanded the switch scale and improved their performance.

This paper reviews recent advances in silica-based PLC switches developed by NTT Photonics Laboratories. First, we provide a brief description of a PLC and describe the basic structure of PLC switch units. We then move on to the configuration and typical performance of  $N \times N$  matrix switches and  $1 \times N$  selection switches. Finally, we review a trial designed to reduce driving power consumption, and mention the reliability of our PLC switch modules.

### 2. Silica-based PLC

The silica-based PLC is an optical circuit with the same structure as an optical fiber that can provide several functions including filtering and switching.

<sup>†</sup> NTT Photonics Laboratories  
Atsugi-shi, 243-0198 Japan  
E-mail: okuno@aecl.ntt.co.jp

Figure 1 shows the process used for fabricating a silica-based PLC switch. This fabrication technique combines flame hydrolysis deposition (FHD) and reactive ion etching (RIE), as used for other silica-based PLCs such as splitters and arrayed waveguide gratings (AWGs) [5]. First, silica glass particles for the under-cladding and core layers are deposited on a silicon substrate by FHD. The basic components are pure silica ( $\text{SiO}_2$ ) for the under-cladding and germanium-doped silica ( $\text{SiO}_2\text{-GeO}_2$ ) for the core. Next, the Si substrate is heated in an electric furnace to consolidate the fine glass particles. Then, unwanted areas of the core layer are removed by photolithography

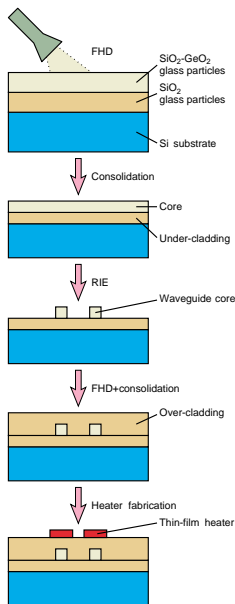


Fig. 1. Fabrication process of silica-based PLC switch.

Table 1. Waveguide parameters used in silica-based PLC switches.

	$\text{H}\Delta$	$\text{SH}\Delta$
Relative refractive index difference (%)	0.75	1.5
Core size ( $\mu\text{m}$ )	6x6	4x4
Propagation loss (dB/cm)	< 0.01	< 0.05
Minimum bending radius (mm)	5	2
Optical fiber coupling loss (dB/point)	0.4	>1

and RIE. After that, the core ridge structures are covered with an over-cladding layer by FHD and consolidated again. Finally, thin film heaters for switching are deposited on the waveguides by the lift-off technique.

PLCs are highly stable and reliable because they have no moving parts, and the waveguide material, silica glass, is physically and chemically stable. In addition, they are suitable for large-scale integration and mass production because they are fabricated by PLC technology. PLCs offer ease of fiber attachment and a low propagation loss, which is lower than 0.01 dB/cm at a wavelength of 1.55  $\mu\text{m}$ , because their material and structure are the same as those of optical fiber. Typical waveguide characteristics for PLC switches are listed in Table 1. Waveguides with a relative refractive index difference  $\Delta$  of 0.75% between the core and cladding (High- $\Delta$ :  $\text{H}\Delta$ ) are mainly used for PLC switches because they have a small minimum bending radius of 5 mm and can be densely integrated. We have been developing optical switches using 1.5%- $\Delta$  waveguides (Super High- $\Delta$ :  $\text{SH}\Delta$ ) with a minimum bending radius of 2 mm to achieve an even higher degree of integration [6].

### 3. Silica-based PLC switch

#### 3.1 Basic configuration

Our basic TO-switch unit is essentially a balanced bridge Mach-Zehnder interferometer (MZI) composed of two 3-dB directional couplers and two waveguide arms, as shown in Fig. 2. The waveguide arms are equipped with thin film heaters on their cladding that operate as TO phase shifters. The optical path length difference  $\Delta nL$  between the two arms is designed to be zero (symmetric-MZI) or a half-wavelength (asymmetric-MZI). The MZI is in the cross-state when  $\Delta nL=0$ : an optical signal is guided from input port 1 to output port 2 or from input port 2 to output port 1. It is in the bar-state when  $\Delta nL$  is the half-wavelength: an optical signal is guided from input port 1 to output port 1 or from input port 2 to

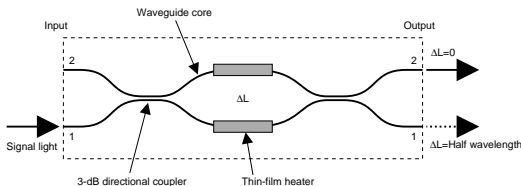


Fig. 2. Basic configuration of silica-based PLC switch.

output port 2. By varying the refractive index of one waveguide arm of the MZI using the TO effect, we can change  $\Delta nL$  by half a wavelength, which changes the switch state. The typical temperature increases at the core and the heater are 15 and 40°C, respectively. The switching power is 0.35 to 0.45 W. The switching time is 1 to 3 ms, which is sufficient for OXC and OADM systems.

### 3.2 N×N matrix switches

Large-scale switches are made by integrating the basic switch units. One such switch is the N×N strictly nonblocking matrix switch<sup>\*1</sup>. We have already developed N×N matrix switches with a scale of up to 16×16 [7]–[12]. Figure 3 shows the configuration of these switches. We use the double-MZI switching units shown in Fig. 3(a) as cross-point switches to obtain a high extinction ratio. The double-MZI switching unit consists of two asymmetric MZI units and an intersection. The optical signals are propagated along the cross-path (from input port 1 to output port 2 or from input port 2 to output port 1) when no driving power is supplied to the TO heater of either MZI unit (OFF-state) or along the bar-path (from input port 1 to output port 1 or from input port 2 to the dummy port) when driving power is supplied simultaneously to the TO heaters of both MZI units (ON-state). In matrix switches, the amount of light leaking from input port 1 to output port 1 in the OFF-state should be kept sufficiently small because it travels to an output port of the matrix switch and increases the crosstalk. The double-MZI switching unit blocks the light leaking at each MZI unit, thus achieving a high extinction ratio: twice that of the basic MZI unit. In

contrast, light leaking from input port 1 to output port 2 in the ON-state is acceptable in terms of crosstalk, because it is ultimately guided to an idle output port of the matrix switch. Figure 3(b) shows the logical arrangement of the N×N matrix switch. This is called the path-independent loss (PI-loss) arrangement, and consists of N switching stages, each with N switching units, and is nonblocking. This arrangement can reduce the total circuit length to half that of the conventional diamond-shaped crossbar arrangement (2N-1) [7]–[9], because it requires half the number of switching stages.

The performance of the fabricated matrix switches is shown in Table 2. Each switch was fabricated using 0.75% $\Delta$  waveguides. The circuit layout of a 16×16 matrix switch is shown in Fig. 3(c). The 100 × 100 mm chip was fabricated on a 6-inch wafer. A total of 256 cross-point switches, corresponding to 512 MZI units, are integrated on one chip. This is the largest number of integrated switches yet achieved in a waveguide-type switch. We have already made 8×8 and 16×16 matrix switch modules. The N×N matrix switch module requires N<sup>2</sup> electrical terminals to feed switching power to each cross-point individually. 256 terminals will be needed in the 16×16 switch module. Since such a large number of terminals makes the module structure complicated, we developed a 16×16 switch module with a driving circuit that has a serial/parallel control signal conversion

Table 2. Performance of fabricated N×N matrix switches.

Switch scale	4×4	8×8	16×16
Chip size (mm <sup>2</sup> )	25×65	68×68	100×100
Waveguide length (cm)	14	29	66
Average insertion loss (dB)	2.6	5.1	5.6
Average extinction ratio (dB)	55	60	59
Power consumption (W)	3	6	13

\*1 nonblocking matrix switch: matrix switch that can guide optical signals through arbitrary optical paths without obstructing other optical paths.

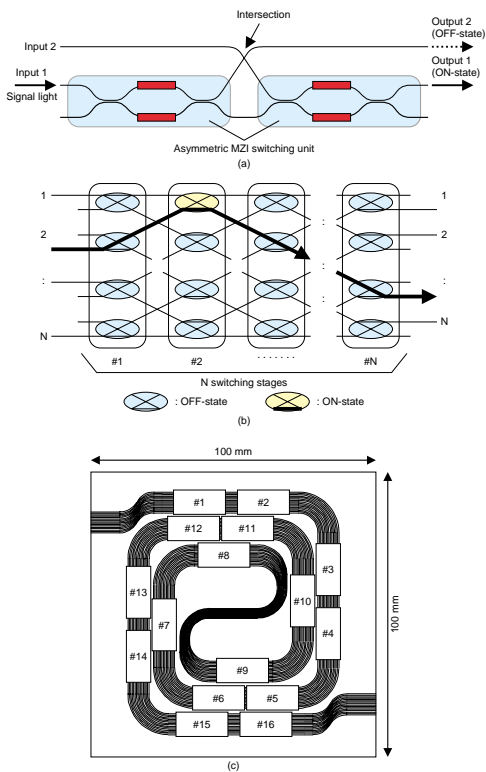


Fig. 3.  $N \times N$  matrix switch: (a) cross-point switching unit (double-gate configuration), (b) logical arrangement (path-independent loss configuration) and (c) circuit layout of 16x16 matrix switch.

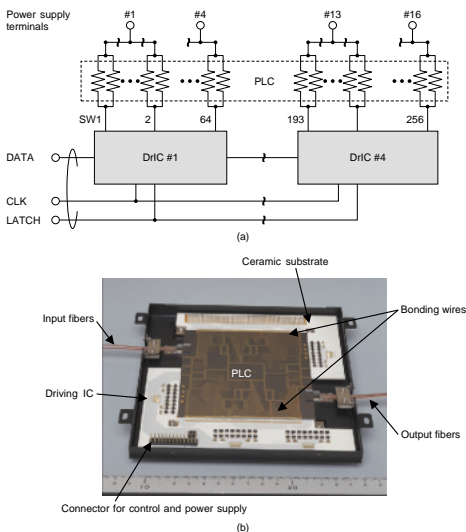


Fig. 4. 16×16 matrix switch module: (a) schematic diagram of the driving circuit and (b) photograph of the module.

function, as shown in Fig. 4(a) [12]. As a result, we were able to reduce the number of electrical terminals to 3 control terminals and 16 power supply terminals. Figure 4(b) is a photograph of a fabricated 16×16 switch module. In this module, the 16×16 switch chip, which was attached to two 16-arrayed fibers, was mounted on a multi-layered ceramic substrate integrated with the driving circuits. The module was  $165 \times 160 \times 23$  mm.

As shown in Table 2, each switch has a low insertion loss and a high extinction ratio, which are the same as those of mechanical switches. Specifically, the insertion loss was reduced by improving the fabrication process, and an average loss of 5.6 dB was achieved in the largest-scale 16×16 switch module. The power consumption was 13 W, which allows air cooling.

### 3.3 1×N switches and their applications

We have also developed 1×N switches that have 1 input port and N output ports. These switches are useful for selecting optical light sources and a signal monitor. We have already made a delivery and coupling switch (DC-SW) for OXC systems that is composed of several 1×N switches and couplers [13].

We adopted two types of logical arrangement for these 1×N switches [14]. One is the tree arrangement, which connects symmetric-MZI units with a binary tree structure, as shown in Fig. 5(a). This is useful for achieving low loss and reducing the chip size because the required number of switching stages is proportional to  $\log N$ . The other is a tap arrangement, which connects asymmetric-MZI units to the main waveguide, as shown in Fig. 5(b). This is useful for achieving low power consumption because only one MZI unit is in the ON-state and all the others are in the

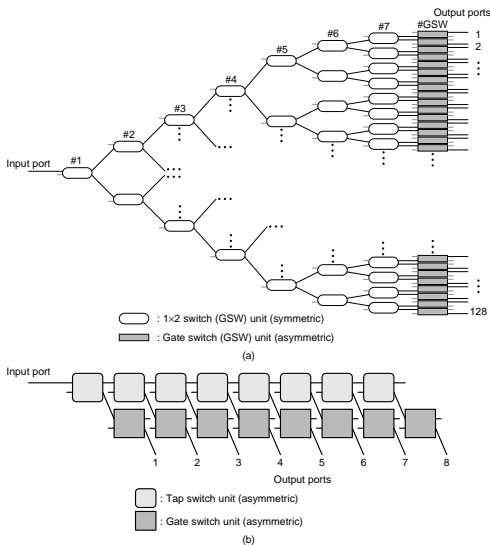


Fig. 5. 1xN switch configurations: (a) tree structure (1x128 switch) and (b) tap structure (1x8 switch).

OFF-state regardless of the switch scale. Both arrangements have additional asymmetric-MZI units in their final stage as gate switches to reduce crosstalk. The gate switch can also be used as an attenuator to adjust the optical output level at the selected output path.

We have fabricated switches ranging from 1x8 to 1x128 [15] with the tree arrangement and a 1x8 switch with the tap arrangement [16]. Table 3 shows the performance of our 1xN switches. The switches not using superhigh $\Delta$  1x128 switch were fabricated using 0.75%-high $\Delta$  waveguides. We obtained a low insertion loss of 2.6 dB even with the 1x128 tree-type switch and a high average extinction ratio of above 50 dB.

These 1xN switches can also be used to construct a large-scale strictly nonblocking NxN switching sub-

system. Figure 6(a) shows the logical arrangement of our 128x128 switching subsystem. This consists of 2N 1xN switch modules and over 16,000 optical fibers. We developed the switch board on which we mounted two 1x128 switch modules, and the subsystem consisted of two 19-inch rack mounts. The fibers that connected the 1x128 switch modules were compactly stored by using a fiber management technique [17] developed in our laboratories. A photograph of the fabricated 128x128 switching subsystem is shown in Fig. 6(b). We fabricated part of this subsystem and measured its performance. The insertion loss was below 6.5 dB (average: 5.7 dB) and the extinction ratio was over 90 dB, proving that this subsystem can be used for large-scale OXC systems.

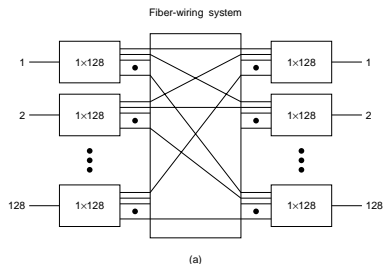


Fig. 6. 128x128 switch subsystem: (a) logical arrangement and (b) photograph of switch subsystem.

Table 3. Performance of fabricated 1xN switches.

Switch scale	1x8 (tree)	1x8 (tap)	1x32 (tree)	1x128 (tree)
Waveguide $\Delta$	H $\Delta$	H $\Delta$	H $\Delta$	SH $\Delta$
Chip size (mm <sup>2</sup> )	18x60	35x74	67x74	60x66
Waveguide length (cm)	6	17	13	11
Average insertion loss (dB)	1.2	1.3	1.5	2.6
Average extinction ratio (dB)	52	56	55	63
Power consumption (W)	1.5	0.5*	2.2	3.5

\*: Switch unit: Low power consumption type

### 3.4 Reconfigurable optical add/drop multiplexer

The silica-based PLC switch can be monolithically integrated with other PLC devices including an AWG multi/demultiplexer because their fabrication processes are the same. We have demonstrated a reconfigurable monolithic 16-channel OADM with athermal operation [18]. The OADM consists of two AWG multi/demultiplexers and an array of 16 2x2 PLC switches as shown in Figs. 7 and 8. The 2x2 switch unit is composed of 4 MZI units to reduce the crosstalk, and 64 MZI units may be activated simultaneously. The refractive index of silica-based waveguides changes with chip temperature, which means such AWG characteristics as center wavelength would also change. To solve the problem in this OADM, we made the AWG characteristics temperature independent by filling grooves formed in the arrayed waveguides with a silicon resin having a negative refractive index temperature dependence that cancels out the positive dependence of the silica-

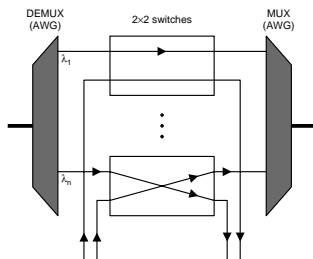


Fig. 7. Configuration of optical add/drop multiplexer.

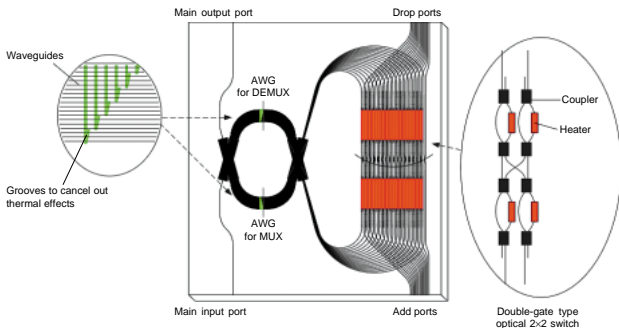


Fig. 8. Circuit layout of OADM.

based waveguides.

Figure 9 shows the transmission spectra from the main input port to the main output port for the 10–80°C temperature range, when the 2<sup>nd</sup>, 5<sup>th</sup>, and 10<sup>th</sup> channels were dropped. We obtained insertion losses below 12 dB and crosstalk below 36 dB. The spectra in Fig. 9 almost all coincide with each other; that is, the characteristics of all the channels are almost completely insensitive to temperature change. Thus, this OADM works stably when there are chip temperature variations caused by changes in the add/drop channel number.

#### 4. Low power consumption technology

The increase in traffic volume means that large-scale and more compact switches are required. We have made larger-scale PLC switches by using 1.5%– $\Delta$  waveguides. Finding a way to reduce the switching power of the MZI unit is very important for larger-scale PLC switches. We have already achieved switching power as low as 90 mW using a Si trench structure and heat-insulating grooves with 0.75%– $\Delta$  waveguides [19]. Moreover, we have already successfully reduced the switching power to 45 mW by

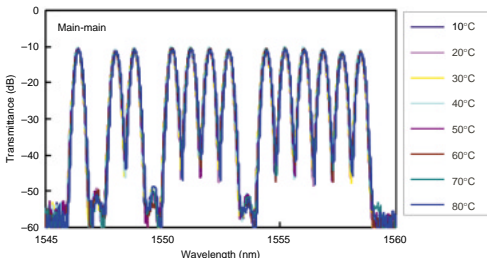


Fig. 9. Transmission spectra of OADM.

using heat-insulating grooves with  $1.5\% \Delta$  waveguides and optimized structural parameters [20].

Figure 10 shows the structure of an MZI switch unit with low power consumption. It has heat-insulating grooves arranged symmetrically with respect to the TO heater. The switching power depends on the thickness of the under-cladding used to suppress heat radiation into the Si substrate and the width of the cladding ridge used to suppress lateral heat diffusion. With a thicker under-cladding, the response time is slower because the heat flow into the Si substrate becomes slower. Therefore, a narrow cladding ridge is much more effective than a thick under-cladding for reducing the switching power while maintaining a reasonable response time. Figure 11 shows the dependence of the experimental switching powers on the cladding ridge width at under-cladding thicknesses of 20 and 50  $\mu\text{m}$ . The solid plots are obtained experimentally, open plots show data for the conventional switches, and the solid lines are theoretical curves. The switching power decreases as the cladding ridge becomes narrower and the under-cladding becomes thicker. We achieved very low switching power of 45 mW with an under-cladding thickness of 50  $\mu\text{m}$  and a cladding ridge width of 20  $\mu\text{m}$ . This power is about one-tenth that of a conventional switch and half that of a conventional low-power-consumption switch [19]. The switching response time was about 3 ms, which is the same as that of the conventional switch. With this low-power MZI, the total power consumption of a  $16 \times 16$  matrix switch should be only 1.4 W.

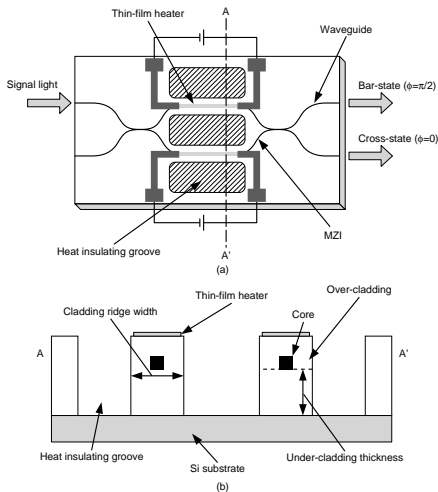


Fig. 10. Structure of low power consumption switch: (a) top view and (b) cross-sectional view.

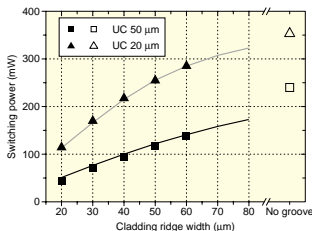


Fig. 11. Dependence of switching power on cladding ridge width.

Table 4. Reliability test results: changes in mean performance value.

Test items	Loss (dB)	Extinction ratio (dB)	Heater resistance (%)	Driving power (%)
Long periods in ON-state (65°C, 5003 h)	-0.2	-1.5	0.0	0.7
Damp heat (75°C, 90%, 5007 h)	0.2	0.9	0.0	-0.2
High temperature (85°C, dry, 5003 h)	-0.1	0.0	0.0	-0.2
Low temperature (-40°C, 2014 h)	0.3	-0.2	0.0	0.2
Heat cycle (-40 to 75°C, 500 cycles)	0.0	-0.4	0.0	0.1
Vibration (20 to 2 kHz, 4 min, 4 cycles)	-0.2	-0.2	0.0	-0.5
Impact (500 G, 6 directions, 5 cycles)	0.0	-0.3	0.0	-0.3

## 5. Reliability

The reliability of PLC devices including fiber connections has been confirmed with splitters and AWGs. Since PLC switches use additional components such as thin-film heaters and power feed electrodes, their reliability must be verified. We carried out a long-term reliability test for switch modules where we also took into account the active conditions [21]. Our test samples were eight arrayed 2×2 switch modules for OADM systems. We performed two categories of test, namely operational and storage tests. Two of the eight arrays of switches were kept in the ON-state in the operational test since the ratio of the add/drop state in a conventional OADM system was 20-30% of all channels. We set the ambient temperature at 65°C to take account of the temperature increase in the cabinet. We carried out six types of storage test: heat-damp, high-temperature, low-temperature, heat-cycle, vibration, and impact tests, in accordance with Telcordia standards. The test results are shown in Table 4. There were no problems such as optimum point drift, heater resistance change, or deterioration in loss and extinction ratio over the 5000-hour duration of the operational test. We also encountered no problems in the ambient temperature and mechanical tests. These results show that silica-based PLC switch modules are highly reliable.

## 6. Conclusion

This paper reported recent progress in silica-based PLC switches. First, we outlined the PLC, N×N matrix switches (up to 16×16), 1×N switches (up to 1×128) and a 128×128 switching subsystem, which combines 1×128 switches. Then, we introduced a monolithic OADM, in which 2×2 switches and AWGs are integrated, and low power consumption technology. Finally, we reported on the reliability of PLC switch modules.

Optical switches are key devices for constructing flexible and low-cost photonic networks, and many types of switches have been developed by many companies. Of these switches, one of the most useful is the silica-based PLC switch, which is highly stable and reliable. PLC switches with many configurations and scales have been made and some integrated switches are already being marketed by an NTT group company. Further advances in PLC switch technology will contribute greatly to the construction of high-performance photonic networks.

## References

- [1] S. Okamoto, M. Koga, H. Suzuki, and K. Kawai, "Robust photonic transport network implementation with optical cross-connect," *IEEE Commun. Mag.*, pp. 94-103, Mar. 2000.
- [2] V. A. Aksyuk, S. Arney, N. R. Basavanahally, D. J. Bishop, C. A. Bolle, C. C. Chang, R. Frahm, A. Gasparyan, J. V. Gates, R. George, C. R. Giles, J. Kim, O. R. Kolodner, T. M. Lee, D. T. Neilson, C. Nijander, C. J. Nuzman, M. Paczkowski, A. R. Papazian, F. Pardo, D. A. Ramsey, R. Ryf, R. E. Scotti, H. Shea, and M. E. Simon, "238 × 238 micromechanical optical cross connect," *IEEE Photon. Technol. Lett.*, Vol. 15, No. 4, pp. 587-589, Apr. 2003.
- [3] M. Makiyama, F. Shimokawa, and K. Kaneko, "Strictly non-blocking N×N thermo-capillary optical matrix switch using silica-based waveguide," *Tech. Dig. OFC2000, TuM2*, pp. 207-209, Baltimore, MD, U.S.A., Mar. 2000.
- [4] J. E. Fouquest, "Compact optical cross-connect switch based on total internal reflection in a fluid-containing planar lightwave circuit," *Tech. Dig. OFC2000, TuM1*, pp. 204-206, Baltimore, MD, U.S.A., Mar. 2000.
- [5] M. Kawachi, "Recent progress in silica-based planar lightwave circuits on silicon," *IEE Proc. Optoelectron*, Vol. 143, No. 5, pp. 257-262, Oct. 1996.
- [6] S. Suzuki, M. Yanagisawa, Y. Hibino, and K. Oda, "High-density integrated planar lightwave circuits using SiO<sub>2</sub>-GeO<sub>2</sub> waveguides with a high refractive index difference," *J. Lightwave Technol.*, Vol. 12, No. 5, pp. 790-796, 1994.
- [7] M. Okuno, A. Sugita, T. Matsunaga, M. Kawachi, Y. Ohmori and K. Kato, "8×8 optical matrix switch using silica-based planar lightwave circuit," *IEICE Transactions on Electronics*, Vol. E76-C, No. 7, pp. 1215-1223, 1993.
- [8] M. Okuno, K. Kato, Y. Ohmori, M. Kawachi, and T. Matsunaga, "Improved 8×8 integrated optical matrix switch using silica-based planar lightwave circuits," *J. Lightwave Technol.*, Vol. 12, No. 9, pp. 1597-1606, 1994.
- [9] M. Okuno, K. Kato, R. Nagase, A. Himeno, Y. Ohmori, and M.

Kawachi, "Silica-based 8x8 optical matrix switch integrated new switching units with large fabrication tolerance," *J. Lightwave Technol.*, Vol. 17, No. 5, pp. 771-781, 1999.

- [10] T. Goh, A. Himeno, M. Okuno, H. Takahashi, and K. Hattori, "High-extinction ratio and low-loss silica-based 8x8 strictly nonblocking thermo-optic matrix switch," *J. Lightwave Technol.*, Vol. 17, No. 7, pp. 1192-1199, 1999.
- [11] T. Goh, M. Yasu, K. Hattori, A. Himeno, M. Okuno, and Y. Ohmori, "Low-loss and high-extinction ratio strictly nonblocking 16x16 thermo-optic matrix switch on 6-inch wafer using silica-based planar light-wave circuit technology," *J. Lightwave Technol.*, Vol. 19, No. 3, pp. 371-379, 1999.
- [12] T. Shibata, M. Okuno, T. Goh, M. Yasu, M. Itoh, M. Ishii, Y. Hibino, A. Sugita, and A. Himeno, "Silica-based 16x16 optical matrix switch module with integrated driving circuits," *Tech. Dig. OFC'2001*, WR1, Anaheim, California, U.S.A., March 2001.
- [13] A. Watanabe, S. Okamoto, M. Koga, K. Sato, and M. Okuno, "Design and performance of delivery and coupling switch board for large scale optical path cross-connect system," *IEICE Trans. Commun.*, Vol. E81-B, No. 6, pp. 1203-1212, Jun. 1998.
- [14] M. Okuno, T. Watanabe, T. Goh, T. Kominato, T. Shibata, T. Kawai, M. Koga, and Y. Hibino, "Low-loss and high-extinction ratio silica-based 1xN thermo-optic switches," *Tech. Dig. OECC/IOOC 2001*, MD5, Sydney, Australia, July 2001.
- [15] T. Watanabe, T. Goh, M. Okuno, S. Sohma, T. Shibata, M. Itoh, M. Kobayashi, M. Ishii, A. Sugita, and Y. Hibino, "Silica-based PLC 1x128 thermo-optic switch," *Proc. of ECOC2001*, TuL.1.2, Amsterdam, The Netherlands, Sep. 2001.
- [16] H. Takahashi, T. Goh, T. Shibata, M. Okuno, Y. Hibino, and T. Watanabe, "High performance 8-arranged 1x8 optical switch based on planar lightwave circuit for photonic networks," *ECOC2002*, 4.2.6, Copenhagen, Denmark, Sep. 2002.
- [17] Y. Abe, M. Kobayashi, M. Hirayama, and R. Nagase, "Large-scale optical fiber wiring for 128x128 PLC switch system with fiber physical contact connectors and optical fiber circuits," *Proc. of 50th IWCS*, pp. 93-97, Lake Buena Vista, Florida, U.S.A., Nov. 2001.
- [18] T. Saida, A. Kaneko, T. Goh, M. Okuno, A. Himeno, K. Takiguchi, and K. Okamoto, "A thermal silica-based optical add/drop multiplexer consisting of arrayed waveguide gratings and double gate thermo-optic switches," *Electron. Lett.*, Vol. 36, No. 6, pp. 528-529, 2000.
- [19] R. Kasahara, M. Yanagisawa, A. Sugita, T. Goh, M. Yasu, A. Himeno, and S. Matsui, "Low-power consumption silica-based 2x2 thermo-optic switch using etched silicon substrate," *IEEE Photon. Technol. Lett.*, Vol. 11, No. 9, pp. 1132-1134, 1999.
- [20] S. Sohma, T. Goh, H. Okazaki, M. Okuno, and A. Sugita, "Low switching power silica-based super high delta thermo-optic switch with heat insulating grooves," *Electron. Lett.*, Vol. 38, No. 3, pp. 127-128, 2002.
- [21] M. Okuno, "Highly integrated PLC-type optical switches for OADM and OXC systems," *Tech. Dig. OFC'2003*, Tu1, Atlanta, Georgia, U.S.A., Mar. 2003.



**Masayuki Okuno**

Senior research engineer, supervisor, Hyper-photonics Component Laboratory, NTT Photonics Laboratories.

He received the B.S., M.S., and Ph.D. degrees in electronic engineering from Hokkaido University, Hokkaido in 1982, 1984, and 2000, respectively. In 1984, he joined NTT Electrical Communications Laboratories, Tokyo, Japan, where he has been engaged in research on optical components and guided-wave optical devices. He is now with NTT Photonics Laboratories, Kanagawa, Japan. He is a member of the IEEE and the Institute of Electronics, Information and Communication Engineers (IEICE) of Japan.



**Takashi Goh**

Research Engineer, Photonic Transport Network Laboratory, NTT Network Innovation Laboratories.

He received the B.S. and M.S. degrees in electronic and communication engineering from Waseda University, Tokyo in 1991 and 1993, respectively. In 1993, he joined the NTT Optoelectronics (now Photonics) Laboratories, Ibaraki, Japan, where he has been engaged in research on silica-based planar lightwave circuits. In 2002, he moved to NTT Network Innovation Laboratories, Kanagawa, Japan and is now engaged in the research and development of optical communication systems. He received the Young Engineer Award from IEICE in 2000. He is a member of the IEICE and the Japan Society of Applied Physics (JSAP).



**Shunichi Sohma**

Researcher, Hyper-photonics Component Laboratory, NTT Photonics Laboratories.

He received the B.S. and M.S. degrees in electronic engineering from Tohoku University, Sendai, Miyagi in 1997 and 1999, respectively. In 1999, he joined NTT Photonics Laboratories, Ibaraki, Japan. He is a member of IEICE. In 2002, he received the Young Researcher Award from the International Conference on Solid State Devices and Materials.



**Tomohiro Shibata**

Senior Research Engineer, Hyper-photonics Component Laboratory, NTT Photonics Laboratories.

He received the B.S. degree in physics, the M.S. degree in applied physics, and the Ph.D. degree in crystalline materials science from Nagoya University, Nagoya in 1983, 1985, and 1995, respectively. In 1985, he joined NTT Laboratories, where he engaged in research on the epitaxial growth of thin film semiconductors utilizing ECR (electron cyclotron resonance) plasma technology. He is now studying the fabrication of silica-based planar lightwave circuits. He is a member of JSAP and the Surface Science Society of Japan.